CHAPTER 4

FINE AGGREGATES AND MORTARS

Fine aggregate, often called sand, is an small inert material in which the particles are less than 5 mm or 3/16" in their size. They can pass through the U.S. standard sieve No. 4. Their major mineral is normally quartz or mica. A good fine aggregate should always be free of organic impurities, clay or any deleterious materials. It primarily functions as a filler inserted in the cavities among coarse aggregate particles. In concrete mix design, the selection of fine aggregate is focused on its gradation, which should be compatible to the coarse aggregate.

The mixture of fine aggregate and cement paste becomes mortar. The inclusion of fine aggregate may improve the properties of the mixture from cement paste alone. Fine aggregate forms the skeleton to carry the internal forces. It is also beneficial to the dimension of stability. However, the presence of fine aggregate makes the mixture demand more water content. There is a tendency of an increase in the porosity. These drawbacks may be reduced by composing the proper gradation and using the relevant amount of sand/cement ratio. As a concrete binder, the improved quality of mortar results in a superior concrete performance.

Thus, in this chapter, the proper gradation of fine aggregate and amount of sand/cement ratio for producing high-strength mortar are analyzed. The additional water content to maintain flow is evaluated. The increase porosity of mortar is also discussed.

4.1 Inclusion of Fine Aggregate

It is obvious that the properties of fine aggregate, as a major component, significantly affect the performance of mortar. These properties include gradation, shape, texture, porosity, strength as well as quantity. Because the fine aggregate particles are too small, the measurement of their individual properties is very difficult. In concrete mix design, only the gradation and amount of fine aggregate are of concern.

4.1.1 Packing Density

There are unlimited numbers of possibilities for composing aggregate gradation, and, in practice, it is impossible to evaluate the effects of all these possibilities. Therefore, the packing density is raised to facilitate this. Packing density is defined as the volume of particles in relation to the total volume of mixture, or, mathematically, as one minus porosity. The packing of aggregate mixtures depends on shape of particles, interaction among particles with different sizes, and degree of compaction.

De Larrard (1999) presented the equation to calculate the actual packing density (ϕ) of n-class aggregate implicitly as:

$$K = \sum_{i=1}^{n} \frac{y_i / \beta_i}{\frac{1}{\phi} - \frac{1}{\gamma_i}} \tag{4.1}$$

where K is the compaction factor, depending on the process of packing. The value of K is 4.1 for pouring, 4.5 for sticking with a rod, and 4.75 with vibration. y_i and β_i are the volume fraction and the residual packing density of class-i aggregate, respectively. And, γ_i is the packing density when class-i aggregate is dominant, and can be computed from:

$$\gamma_i = \frac{\beta_i}{1 - \sum_{j=1}^{i-1} \left[1 - \beta_i + b_{ij}\beta_j \left(1 - 1/\beta_j\right)\right] y_j - \sum_{j=i+1}^{n} \left[1 - a_{ij}\,\beta_i / \beta_j\right] y_j} \tag{4.2}$$

where a_{ij} and b_{ij} are the parameters representing interaction between each class of particles, i.e. loosening and wall effect, respectively. Both coefficients are function of the ratio between the diameter of class-i and -j particle, as

$$a_{ij} = \sqrt{1 - \left(1 - d_j / d_i\right)^{1.02}} \tag{4.3}$$

$$b_{ij} = 1 - \left(1 - d_i / d_j\right)^{1.50} \tag{4.4}$$

The calculation above can be easily implemented in the computer program. Then, the variation of packing density of aggregate mixtures with various patterns of gradation is readily determined.

To illustrate this calculation, the ordinary river sands from two sources are used. Their original fineness modulus is 2.80 and 2.94. They are classified by retaining on the U.S. standard

sieves (No.4 to No.100). The unit weight and void content between particles of each group is measured according to the standard test method of ASTM C29. The residual packing density (β) can be then computed implicitly by using eq. (4.1) and setting i =1, i.e.,

$$K = \frac{1}{\beta/\phi - 1} \tag{4.5}$$

Because, in ASTM C29 the fine aggregate is compacted by sticking with a rod, K in eq. (4.5) equals to 4.5. Table 4.1 shows the test results and the calculated residual packing density for fine aggregate with each size. For both fine aggregates, the unit weight increases with size reduction, while void content decreases. The actual packing density varies from 0.56 to 0.60, whereas the residual packing density is in the interval of 0.68 to 0.73.

Five gradation patterns presented in Fig. 4.1 are used for calculating the actual packing density. The first one, with fineness modulus of 2.15, is the upper bound of the suggested gradation according to ASTM C33. At the other end, the last one with a fineness modulus of 3.33 is the lower bound. The remainders lie between these two extremes. The Fuller's ideal gradation and single-size gradation are also added. The values of packing density are shown in Table 4.2. It can be seen that the Fuller's ideal gradation yields the maximum packing density, while among the gradation conforming to ASTM, the packing density of gradation pattern No. 4 (FM = 3.04) is the highest.

4.1.2 Distance between Particles

Where the packing density is concerned, an aggregate particle is in contact with the others. But, indeed, the particles need a layer of binder to coat around them. The thickness of the coating or the distance between particles means the amount of required aggregate in the mixture. Fig. 4.2 shows the relation between sand/cement ratio and the thickness of coating for the given patterns of gradation. It can be observed that the graphs of the suggested gradations following to ASTM C33 are very closed. For a specific sand/cement ratio, the coating thickness of the mixture with a single-size fine aggregate is less than that of the others, whereas the Fuller's ideal gradation provides the highest one.

The distance between particles also influences the flow of the mixture, i.e. the shorter spacing, the lower consistency. Therefore, the mortar with single-size fine aggregate yields poor workability. Because the gradation of ASTM C33 is derived from the workability viewpoint, the

curves of the suggested gradation in Fig. 4.2 may represent the boundary of the coating thickness for satisfactory flow. With this in mind, the Fuller's ideal curve is the perfect one because it provides both sufficient packing density and coating thickness.

4.1.3 Simulation of Mortar Strength

Because fine aggregate is generally much stronger than cement paste, mortar with greater value of packing density of fine aggregate is prefered. However, the thickness of coating cement paste should be optimized. Inadequate thickness causes stress concentration at the aggregate surface, whereas excessive coating makes the mortar weaker.

Thus, in this section, the influence of fine aggregate on mortar strength is investigated by using the micro-mechanical model presented in chapter 2. Seven gradation patterns in the previous section are applied. The coating thickness varies in the term of sand/cement ratio, i.e. from 0 to 3.5. Three simulations are done for each sample with different generated aggregate arrangements. The example of aggregate configuration is illustrated in Fig. 4.3. Fine aggregate is assumed to be linear elastic. The elastic modulus and Poisson's ratio of quartz mineral are assigned to the sand, i.e. 60 GPa and 0.18 (Pirsson and Knopf, 1952), respectively. The properties of cement paste are tabulated in Table 4.3. Three levels of paste tensile strength are considered.

The results from the simulations are shown in Table 4.4, and the average ratio of the simulated mortar strength to paste strength (sand/cement ratio equals to 0) is plotted in Fig. 4.4. It can be seen that mortar strength tends to increase with increasing sand content until the peak is reached at sand/cement ratio approximately 2.5, except for the mortar with single-size fine aggregate where the zenith is at sand/cement ratio of 2.0. It can be observed from Fig. 4.2 that these values of sand/cement ratio provide the critical coating thickness of about 0.20 times the radius of fine aggregate.

The graph also shifts when the gradation pattern changes. The same as expected from the packing density, Fuller's ideal gradation provides the highest mortar strength and single-size gradation results in the lowest one, for all value of sand/cement ratio. Among the mortars with ASTM gradation, there is a little increase when the fineness modulus is reduced. This is because cracks propagate around fine aggregate particles. Thus, with the mortar of fine sand, i.e. high surface area, it can sustain load more than the mortar with coarse sand. However, when the sand content is too much, this discrepancy becomes insignificant.

4.1.4 Additional Water Content

A fine aggregate provides a high specific surface area. It requires more mixing water to wet all particles and maintain the flow of the mixture. From the concept of free water (Stitmannaitham, 1992), the retained water from fine aggregate is the product of the mass of fine aggregate and its coefficient of retaining (β_S). Kitticharoenkiat (1998) presented an equation to evaluate this coefficient as

$$\beta_S = \left(2\times10^{-6}\right) SS_F^{0.92} \tag{4.6}$$

where SS_F is the specific surface area of fine aggregate in the unit of cm^2/kg. Because fine aggregate particle is not perfectly round, the angularity factor (Ψ_F) is raised to correct the calculation of the specific surface area, that is

$$SS_F = \frac{SS_{F,o}}{\Psi_F} \tag{4.7}$$

where $SS_{F,o}$ is the specific surface area of the ideal sphere and is an inverse function of the average diameter. Loudon (1953) proposed the expression of angularity factor as

$$\Psi = 1 + 4.44\left(\varepsilon - 0.42\right) \tag{4.8}$$

where ε is void content of the aggregate in loose condition.

4.2 Gradation and Fineness Modulus

The simulation results in the previous section show that difference in packing density and specific surface area of fine aggregate, owing to the various gradation patterns, yields a different load-carrying performance of the mortar. In addition, mortar with Fuller's ideal fine aggregate seems to be the most preferred where the mortar strength is concerned. However, the presence of fine aggregate also influences other mortar properties, such as flow and porosity. Thus, seven gradation patterns used for those simulations are investigated experimentally here.

The same type-I portland cement as in chapter 3 is used with water/cement ratio of 0.20, while the classified ordinary sands in section 4.1 are applied as fine aggregate with sand/cement ratio of 2.0. They are re-blended to obtain the specified gradation. The polymer-based superplasticizer is added for providing flow value of 110% ±5%. The mix proportions are shown in Table 4.5. The designation of M20-F215 represents the mortar mix with water/cement ratio of

0.20 and fineness modulus of 2.15. Cement and sand are mixed in a dry condition for 30 seconds before the same specimen preparation as for cement paste is applied.

It can be observed that the additional amount of superplasticizer for mortar with fine aggregate conforming ASTM C33 is in between 2% and 4%, while that of mortar with Fuller's ideal fine aggregate and with single-size fine aggregate is up to 8% and 10%, respectively. Though Fuller's ideal fine aggregate yields the low value specific surface area, but the large proportion of its coarse grains results in low flow value possibly due to aggregate interlocking.

The measured unit weight and air content of fresh mortar are tabulated in Table 4.6. The average unit weight is about 2445 kg/m^3, while air content varies from 2.81% to 4.21%. Fig. 4.5 shows the plot of total porosity of hardened mortar. For all ages, the total porosity of mortar with single-size fine aggregate is the highest, followed by the mortar containing Fuller's ideal fine aggregate. It may be caused by its low initial flow. Among mortars with ASTM sand, the mortar with fineness modulus of 3.04 yields the slightly lowest total porosity, i.e. 9.54%, 8.61%, 8.26% and 8.12% at 7, 28, 56 and 91 days, respectively. The trend of total porosity with gradation pattern seems to be opposite to the packing density.

The test results for compressive strength are presented in Fig. 4.6. It is reciprocal of total porosity. That is, the compressive strength of the mortar with fineness modulus of 3.04 is the highest one for all ages. They are 98.63, 126.57, 134.78 and 136.37 at 7, 28, 56 and 91 days, respectively. In addition, the compressive strength of the mortar containing Fuller's fine aggregate and single-size fine aggregate are considerably lower than the others. The ratio of mortar strength to cement paste strength is in the range of 1.04 and 1.27. It is lower than that predicted by the simulation. This will be discussed later. Further, the ratio of mortar strength to paste strength decreases when the age of mortar increases.

From the above results, the following conclusions can be drawn. Fine aggregate used to make high-strength mortar should have the grain size distribution within the limits recommended by the ASTM C33. Beyond these limits, the workability of fresh mortar is poor. However, the gradation should lie on the coarser side of such limits, i.e. fineness modulus about 3.0. It is beneficial in the improvement of workability and the reduction of water requirement. Moreover, the required paste volume is diminished. Consequently, the porosity of mortar is low while the strength is high.

4.3 Optimized Sand/Cement Ratio

The simulation also shows that there is an optimum sand/cement ratio, corresponding to a critical average thickness of cement paste covering fine aggregate particles for the maximum mortar strength. However, such critical thickness may not be achieved in practice because the workability of mortar may not be sufficient to compact the mixture well, and cause the mortar strength to not develop completely. In this section, the effect of covering paste thickness or sand/cement ratio is investigated from the experiment.

The mortar from the previous section that contains fine aggregate with fineness modulus of 3.04 is reproduced here, but the sand/cement ratio is varied from 1.0 to 3.0. The mortar flow is controlled as usual. The mix proportions are shown in Table 4.9. To be an example, the extension of -SC10 represents the mortar mix with sand/cement ratio of 1.0. It should be noted that the percent addition of superplasticizer increases with sand/cement ratio. It is 2.0% for sand/cement ratio of 1.0, and 6.0% for sand/cement ratio of 3.0.

The unit weight and air content of the fresh mortar are shown in Table 4.10. Unit weight varies from 2409 to 2461 kg/m^3, and air content is about 2%-4%. Both of them increase with increasing sand/cement ratio. The total porosity of hardened mortar is shown in Fig. 4.7. It can be seen that the mortar with sand/cement ratio of 2.0 provides the minimum total porosity for all ages, i.e., 9.54, 8.61, 8.26 and 8.12 at 7, 28, 56 and 91 days, respectively. The compressive strength of hardened mortar at each age is shown in Fig. 4.8. The inverse trend to the total porosity is obtained. The compressive strength of the mortar with sand/cement ratio of 2.0 is the highest. They are 98.63, 126.61, 134.78 and 136.37 MPa at 7, 28, 56 and 91 days, respectively.

When compared to the results from the simulation, the ratio of mortar strength to cement paste strength from the experiment is lower for all values of sand/cement ratio. It may be because some conditions, which are assumed for aggregate arrangement, are missing. That is, the additional porosity is included in the mortar due to the presence of fine aggregate. Table 4.13 demonstrates the ration of the 28-day total porosity to each component of mortar. The total porosity of cement paste with water/cement ratio of 0.20 that measured in chapter 3 is used here for calculating the porosity in paste component, while the percent of water absorption represents the porosity in fine aggregate. An increase in sand/cement ratio reduces the percent of paste volume. Then, the total porosity tends to decrease in the paste component, but increase in fine

aggregate phase. The remaining porosity is assumed to be the additional porosity due to the existence of fine aggregate. It can be seen that this porosity increases with increasing sand/cement ratio, i.e., from 1.47% for mortar with sand/cement ratio of 1.0 to 6.89% for mortar with sand/cement ratio of 3.0.

To account for the additional porosity in mortar, sets of simulations are repeated with some elements, of which the mechanical properties are assigned to be null, representing a void space in the cement paste phase. This rising porosity varies from 2% to 8% of mortar area. The ratio mortar strength to paste strength from the simulations is shown in Fig. 4.9, as well as that obtained from the experiment at 28 days. It is obvious that mortar strength drops, when the porosity is introduced, and the more porosity, the less strength. For the given porosity, this reduction increases with sand content. Further, the optimum sand/cement ratio for the highest mortar strength shifts from 2.5 to 2.0 when the additional porosity becomes 8%. In practice, the total porosity depends on sand/cement ratio. Therefore, the compressive strength of mortar with higher fine aggregate content is considerably reduced.

It can be concluded in this section that, for a given gradation pattern of fine aggregate, there is an optimum sand/cement ratio or percent of paste volume so that the mortar strength is maximum. Less than this value, the strength of mortar can not develop fully because of an insufficient amount of fine aggregate. On the other hand, beyond this point, the surplus fine aggregate induces much porosity into the mortar microstructure, causing deterioration of mortar strength. Sand/cement ratio of 2.0 is found to be appropriate for producing high-strength mortar, when the mortar flow is guaranteed.

4.4 Change in Optimized Water/Cement Ratio

From chapter 3, it is seen that the water/cement ratio about 0.16 yields the best performance for hardened cement paste. But, in the case of mortar, some water is held by the particles of fine aggregate. The net water content involved in the chemical reaction is reduced. Thus, there is a shift in the optimum water/cement ratio.

Thus, in this section, mortar specimens with fine aggregate conforming ASTM C33, fineness modulus of 3.04 and sand/cement ratio of 2.0 are produced by varying water/cement

ratio from 0.12 to 0.28. The flow value of 110% ±5% is still guaranteed by adding superplasticizer. The mix proportions are shown in Table 4.15.

Table 4.16 shows the measured unit weight and air content of the fresh mortar. The unit weight is approximately 2335 kg/m^3 at water/cement ratio of 0.28. It rises with reducing water/cement ratio and is about 2584 kg/m^3 at water/cement ratio of 0.12. The air content of most mortar mixes is less than 4.0%. Compared to cement paste, the air content of about 2.0% is introduced into the mixtures due to the presence of fine aggregate, when the flow value is kept constant.

The total porosity of hardened mortar is plotted with water/cement ratio in Fig. 4.10. The measured total porosity varies between 8.12% to 13.14%. It decreases when the mortar grows. The water/cement ratio of 0.20 yields the lowest total porosity. Fig. 4.11 shows the graph of compressive strength of mortar against water/cement ratio. The highest compressive strength is found in the mortar with water/cement ratio of 0.20. It seems that the optimum water/cement ratio shifts from 0.16 for cement pate to 0.20 for mortar.

By using the concept of free water, the coefficient of retaining of fine aggregate (β_S) can be calculated from eq. (4.6). With the using sand, of which the specific surface area is 15737 cm^2/kg, the β_S coefficient is 0.01277. That is, the additional water content is about 1.3% of sand content. Therefore, in this experiment, the effective water/cement ratio for hydration reaction is reduced by approximately 0.03 for each mix. This reducing water content possibly makes change in the optimum water/cement ratio for the maximum mortar strength.

Table 4.1 Packing density of fine aggregates with various sizes

Passing Seive		Sand A				Sand B			
No.	Max. Diam. (mm.)	Unit Weight (kg/m^3)	Void Content (%)	Actual Packing Density	Residual Packing Density	Unit Weight (kg/m^3)	Void Content (%)	Actual Packing Density	Residual Packing Density
3/8"	9.50	1564	43.98	0.5602	0.6847	1581	43.24	0.5676	0.6938
4	4.75	1573	43.48	0.5652	0.6908	1586	43.14	0.5686	0.6950
8	2.36	1595	42.70	0.5730	0.7003	1616	42.04	0.5796	0.7084
16	1.18	1604	42.61	0.5739	0.7014	1627	41.76	0.5824	0.7118
30	0.60	1613	42.24	0.5776	0.7059	1640	41.36	0.5864	0.7167
50	0.30	1622	41.95	0.5805	0.7095	1656	40.56	0.5944	0.7265
100	0.15	1634	41.53	0.5847	0.7146	1662	40.60	0.5940	0.7260

Table 4.2 Properties of fine aggregate with various gradation patterns

Seive		Cumultive Percent Passing						
No.	Max. Diam. (mm.)	Gradation Pattern						
		No. 1 (Upper bound)	No. 2 (3rd Quartile)	No. 3 (2nd Quartile)	No. 4 (1st Quartile)	No. 5 (Lower Bound)	No. 6 (Fuller's Ideal)	No. 7 (Single Size)
3/8"	9.50	100.00	100.00	100.00	100.00	100.00	100.00	100.00
4	4.75	100.00	98.75	97.50	96.25	95.00	70.71	100.00
8	2.36	100.00	95.00	90.00	85.00	80.00	49.84	100.00
16	1.18	85.00	76.25	67.50	58.75	50.00	35.24	100.00
30	0.60	60.00	51.25	42.50	33.75	25.00	25.13	0.00
50	0.30	30.00	25.00	20.00	15.00	10.00	17.77	0.00
100	0.15	10.00	8.00	6.00	4.00	2.00	12.57	0.00
Fineness Modulus		2.15	2.45	2.74	3.04	3.33	3.01	3.00
Specific Surface Area (cm^2/kg)		33962	24479	19135	15737	13320	14257	25929
Packing Density: Sand A		0.6791	0.6853	0.6896	0.6809	0.6872	0.7185	0.5876
Sand B		0.6869	0.6920	0.6956	0.6964	0.6927	0.7256	0.5964

Table 4.3 Parameters for simulating compressive behavior of mortars

Phase	Simulation	E (GPa)	f_t (MPa)	G_F (N/mm)	ν
Fine Agg.	All	60.0	-	0.07	0.18
Cement Paste	1	18.0	3.0	0.05	0.25
	2	27.0	4.0	0.05	0.25
	3	36.0	5.0	0.05	0.25

Table 4.4 Results of the simulations

Simulation No. 1							
s/c ratio	Average Compressive Strength (MPa)						
	FM = 2.15	FM = 2.45	FM = 2.74	FM = 3.04	FM = 3.33	Fuller's	Single Size
0.0	548.2	548.2	548.2	548.2	548.2	548.2	548.2
0.5	588.8	588.3	587.7	587.2	586.1	596.3	580.2
1.0	640.9	637.2	635.0	632.3	629.1	649.5	620.5
1.5	685.5	681.2	676.4	671.0	667.2	695.7	656.5
2.0	719.4	715.6	711.3	706.5	701.6	730.6	686.1
2.5	740.3	736.6	732.3	728.5	724.2	753.2	683.9
3.0	734.9	731.7	728.0	724.2	721.0	746.8	677.5
3.5	716.7	715.1	714.0	711.8	710.2	724.7	666.2

Simulation No. 2							
s/c ratio	Average Compressive Strength (MPa)						
	FM = 2.15	FM = 2.45	FM = 2.74	FM = 3.04	FM = 3.33	Fuller's	Single Size
0.0	726.3	726.3	726.3	726.3	726.3	548.2	548.2
0.5	811.9	811.2	810.5	809.7	808.2	620.7	603.9
1.0	883.8	878.6	875.7	872.0	867.5	676.0	645.8
1.5	945.3	939.4	932.7	925.3	920.1	724.1	683.3
2.0	992.0	986.8	980.9	974.2	967.5	760.5	714.1
2.5	1020.9	1015.7	1009.7	1004.6	998.6	783.9	711.8
3.0	1013.4	1009.0	1003.8	998.6	994.2	777.2	705.1
3.5	988.3	986.0	984.6	981.6	979.4	754.3	693.4

Simulation No. 3							
s/c ratio	Average Compressive Strength (MPa)						
	FM = 2.15	FM = 2.45	FM = 2.74	FM = 3.04	FM = 3.33	Fuller's	Single Size
0.0	918.0	918.0	918.0	918.0	918.0	918.0	918.0
0.5	1006.1	1005.2	1004.3	1003.4	1001.5	1019.0	991.4
1.0	1095.2	1088.7	1085.1	1080.5	1075.0	1109.9	1060.3
1.5	1171.4	1164.0	1155.8	1146.6	1140.2	1188.8	1121.8
2.0	1229.2	1222.8	1215.4	1207.2	1198.9	1248.5	1172.3
2.5	1265.0	1258.6	1251.2	1244.8	1237.5	1287.0	1168.6
3.0	1255.8	1250.3	1243.9	1237.5	1232.0	1276.0	1157.6
3.5	1224.6	1221.9	1220.0	1216.4	1213.6	1238.4	1138.3

Table 4.5 Mix proportion of mortar with various gradation patterns

Designation	Cement (kg/m^3)	Water (kg/m^3)	Sand (kg/m^3)	Superplasticizer (kg/m^3)
M20-F215	779	156	1558	31
M20-F245	779	156	1558	31
M20-F274	779	156	1558	23
M20-F304	779	156	1557	23
M20-F333	779	156	1558	16
M20-F301	779	156	1558	62
M20-F300	779	156	1559	78

Table 4.6 Fresh properties of mortar with various gradation patterns

Designation	Unit Weight (kg/m^3)	Air Void (%)
M20-F215	2445	3.15
M20-F245	2453	2.81
M20-F274	2431	3.36
M20-F304	2440	2.98
M20-F333	2427	3.22
M20-F301	2447	4.21
M20-F300	2473	3.86

Table 4.7 Total porosity of mortar with various gradation patterns

Designation	Total Porosity (%)			
	7 days	28 days	56 days	91 days
M20-F215	11.19	9.67	9.13	8.83
M20-F245	10.48	9.21	8.90	8.64
M20-F274	9.75	8.89	8.41	8.35
M20-F304	9.54	8.61	8.26	8.12
M20-F333	9.93	9.03	8.72	8.59
M20-F301	13.63	12.42	11.94	11.70
M20-F300	14.48	13.08	12.73	12.58

Table 4.8 Compressive strength of mortar with various gradation patterns

Designation	Compressive Strength (MPa)			
	7 days	28 days	56 days	91 days
M20-F215	92.11	118.50	128.82	130.49
M20-F245	95.44	121.46	129.59	133.16
M20-F274	97.12	124.81	132.13	135.55
M20-F304	98.63	126.57	134.78	136.37
M20-F333	94.15	120.82	130.18	132.69
M20-F301	84.36	107.34	116.29	125.60
M20-F300	81.29	104.80	118.62	123.19

Table 4.9 Mix proportion of mortar with various sand/cement ratio

Designation	Cement (kg/m^3)	Water (kg/m^3)	Sand (kg/m^3)	Superplasticizer (kg/m^3)
M20-SC10	1110	222	1110	22
M20-SC15	915	183	1373	23
M20-SC20	779	156	1557	23
M20-SC25	678	136	1694	27
M20-SC30	600	120	1799	36

Table 4.10 Fresh properties of mortar with various sand/cement ratio

Designation	Unit Weight (kg/m^3)	Air Void (%)
M20-SC10	2409	2.24
M20-SC15	2421	2.93
M20-SC20	2440	2.98
M20-SC25	2453	3.19
M20-SC30	2461	3.66

Table 4.11 Total porosity of mortar with various sand/cement ratio

Designation	Total Porosity (%)			
	7 days	28 days	56 days	91 days
M20-SC10	10.61	9.54	9.03	8.73
M20-SC15	9.85	8.93	8.48	8.38
M20-SC20	9.54	8.61	8.26	8.12
M20-SC25	10.88	9.09	8.82	8.53
M20-SC30	12.61	10.31	9.63	9.16

Table 4.12 Compressive strength of mortar with various sand/cement ratio

Designation	Compressive Strength (MPa)			
	7 days	28 days	56 days	91 days
M20-SC10	90.14	117.70	126.60	131.45
M20-SC15	95.21	123.98	130.11	133.59
M20-SC20	98.63	126.61	134.78	136.37
M20-SC25	94.60	122.86	128.40	130.60
M20-SC30	86.12	112.84	120.93	125.18

Table 4.13 28-day total porosity in each component of mortar with various sand/cement ratio

Designation	Total Porosity (%)			
	All	In Paste	In Sand	Additional
M20-SC10	9.54	7.85	0.22	1.47
M20-SC15	8.93	6.48	0.27	2.19
M20-SC20	8.61	5.51	0.30	2.80
M20-SC25	9.89	4.82	0.33	4.74
M20-SC30	11.51	4.27	0.35	6.89

Table 4.14 Ratio of mortar to paste strength from simulations and experiment

s/c ratio	Average Mortar Strength to Paste Strength					
	Pors. 0%	Pors. 2%	Pors. 4%	Pors. 6%	Pors. 8%	Test
0.0	1.000	0.996	0.992	0.983	0.974	1.000
0.5	1.093	1.078	1.062	1.041	1.019	
1.0	1.177	1.151	1.124	1.092	1.059	1.162
1.5	1.249	1.217	1.185	1.142	1.098	1.224
2.0	1.315	1.273	1.232	1.179	1.127	1.250
2.5	1.356	1.304	1.252	1.189	1.125	1.213
3.0	1.348	1.286	1.224	1.154	1.084	1.114
3.5	1.325	1.257	1.188	1.111	1.034	

Table 4.15 Mix proportion of mortar with various water/cement ratio

Designation	Cement (kg/m^3)	Water (kg/m^3)	Sand (kg/m^3)	Superplasticizer (kg/m^3)
M28	733	205	1466	7
M24	755	181	1511	11
M20	779	156	1558	23
M16	804	129	1608	56
M12	831	100	1661	91

Table 4.16 Fresh properties of mortar with various water/cement ratio

Designation	Unit Weight (kg/m^3)	Air Void (%)
M28	2325	3.61
M24	2366	3.76
M20	2440	3.30
M16	2503	3.60
M12	2591	3.42

Table 4.17 Total porosity of mortar with various water/cement ratio

Designation	Total Porosity (%)			
	7 days	28 days	56 days	91 days
M28	11.16	10.12	9.63	9.15
M24	9.93	9.32	8.71	8.43
M20	9.54	8.61	8.26	8.12
M16	10.12	9.48	8.83	8.39
M12	13.14	11.68	11.02	10.69

Table 4.18 Compressive strength of mortar with various water/cement ratio

Designation	Compressive Strength (MPa)			
	7 days	28 days	56 days	91 days
M28	85.63	109.18	116.93	122.67
M24	91.13	115.30	127.15	132.11
M20	98.63	126.57	134.78	136.37
M16	95.15	122.44	130.11	131.69
M12	77.11	103.06	109.82	114.51

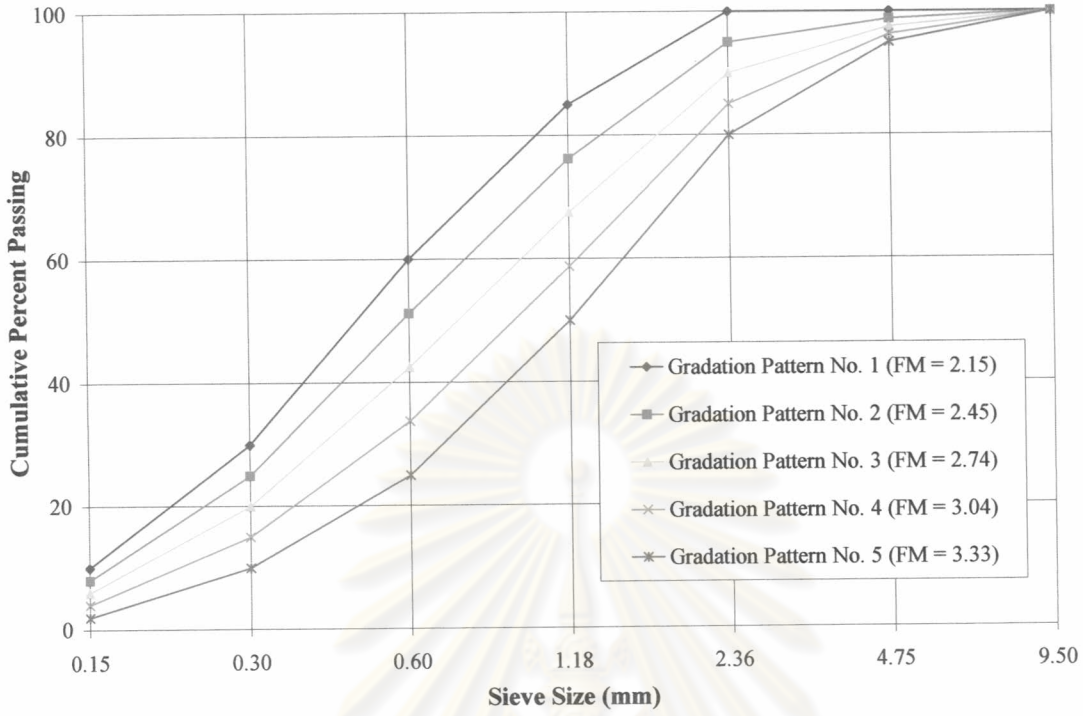

Fig. 4.1 Gradation patterns for illustrating packing density

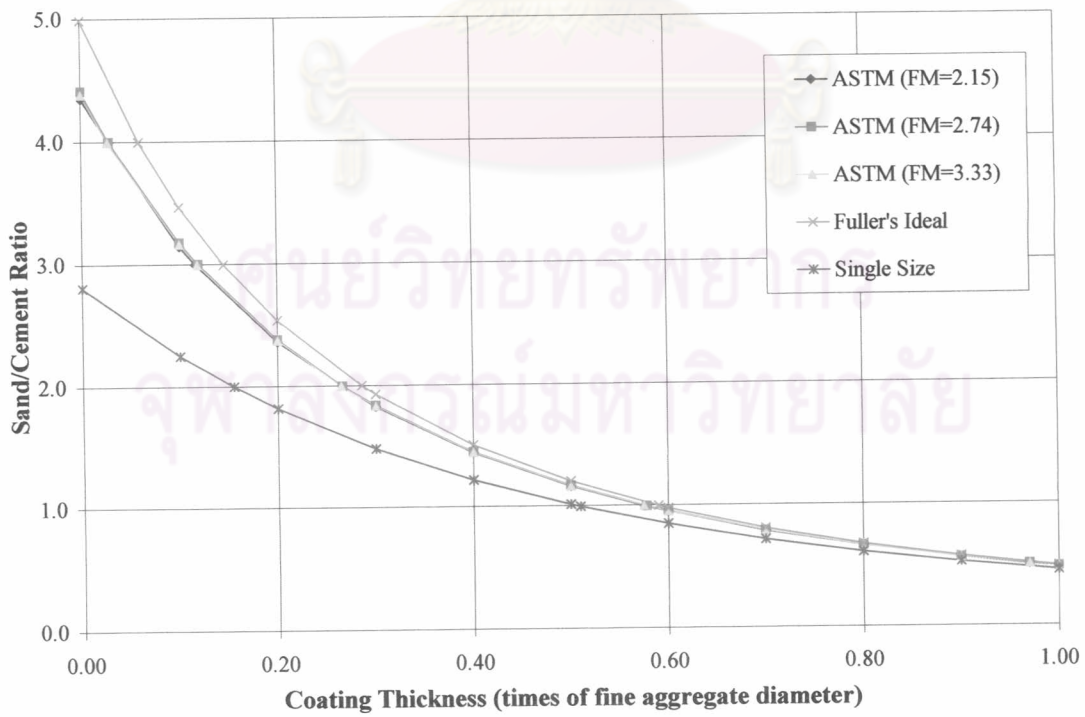

Fig. 4.2 Coating thickness of paste against sand/cement ratio

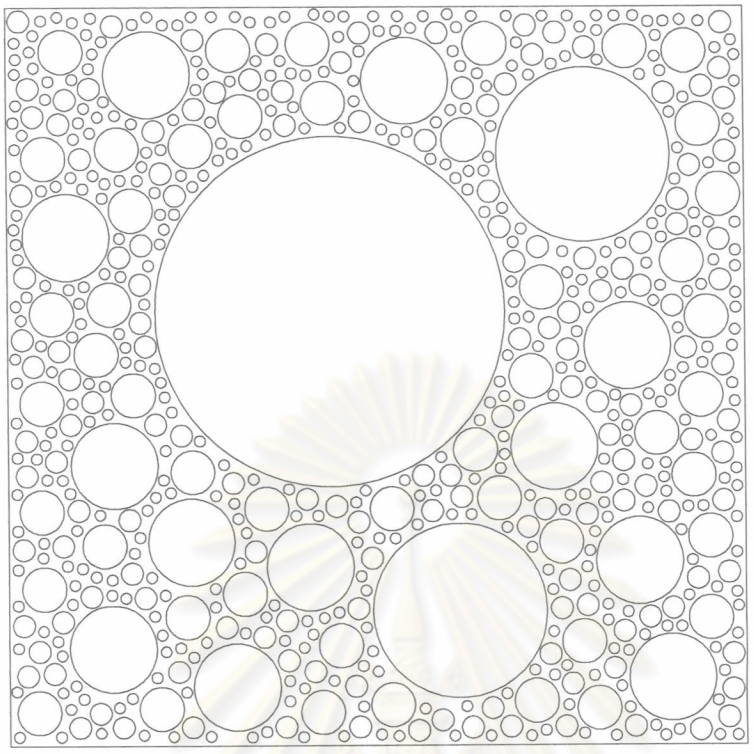

Fig. 4.3 Example of fine aggregate arrangement for the simulation (FM=2.74, s/c=2.0)

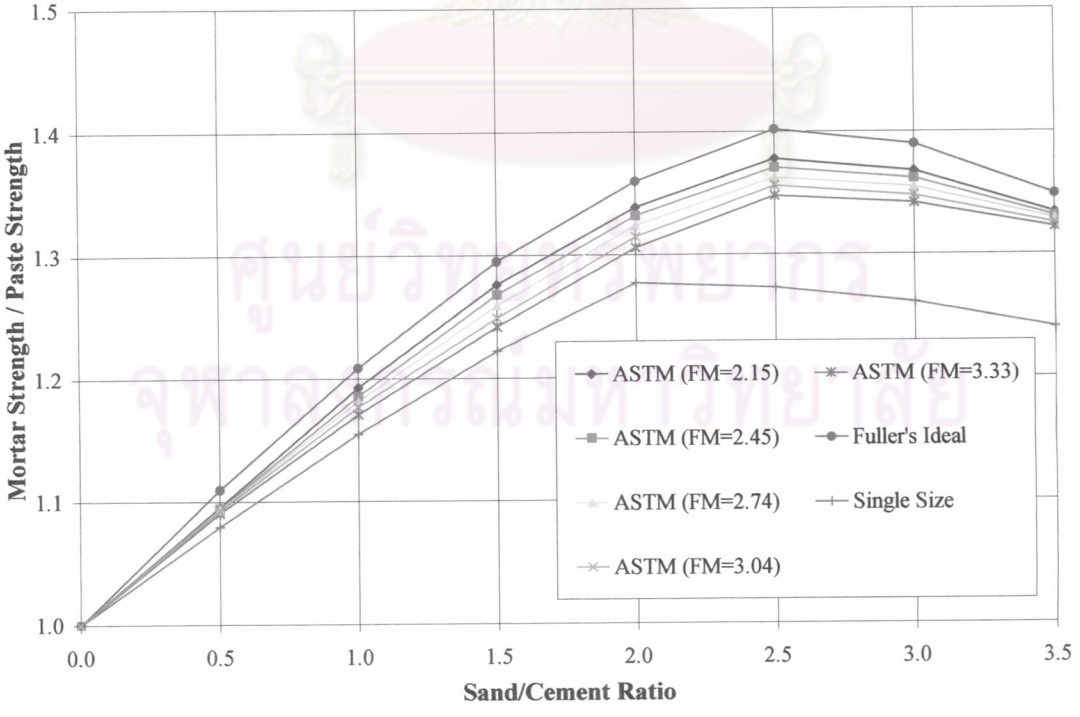

Fig. 4.4 Simulated normalized mortar strength against sand/cement ratio with various gradations

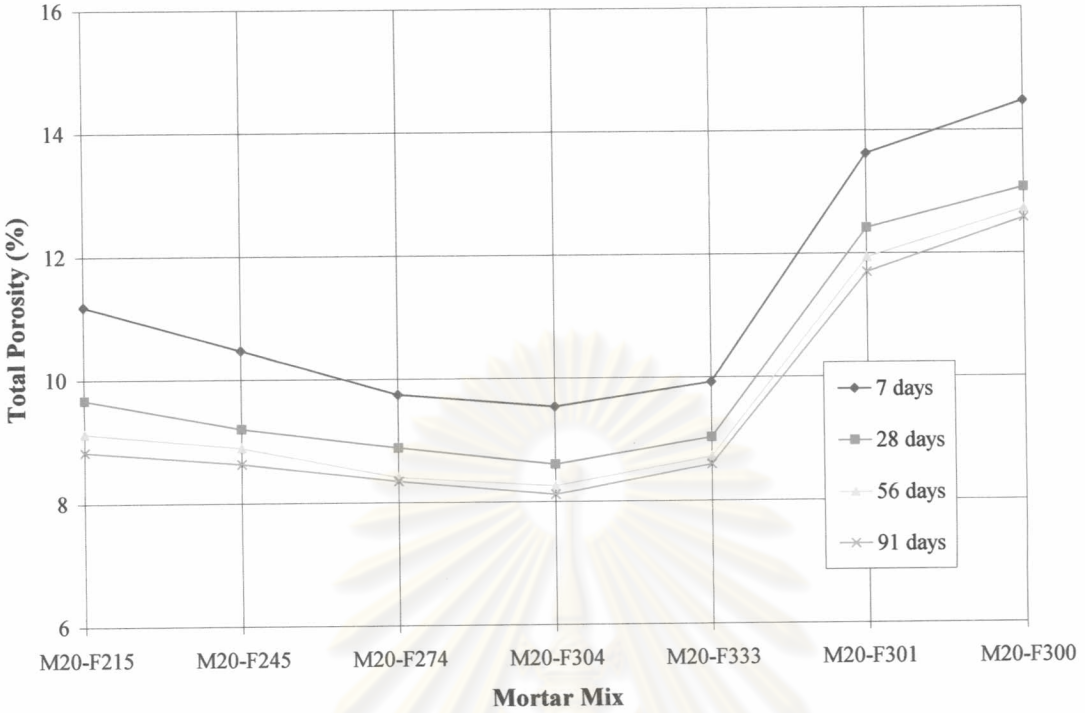

***Fig. 4.5** Total porosity of mortar with various gradation patterns*

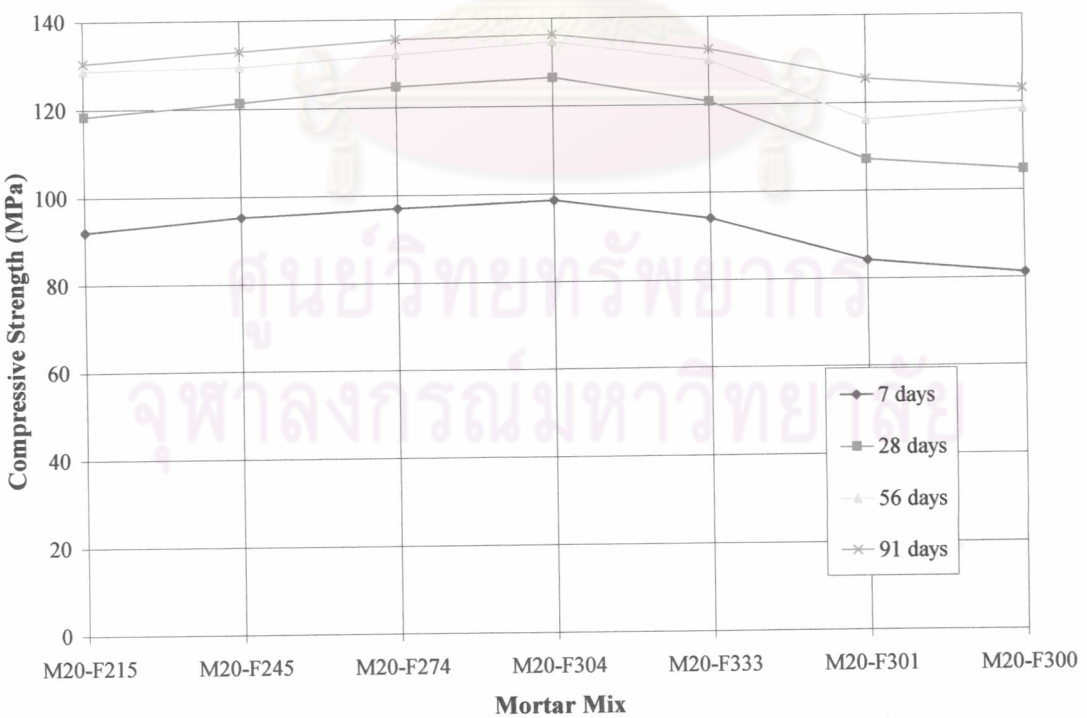

***Fig. 4.6** Compressive strength of mortar with various gradation patterns*

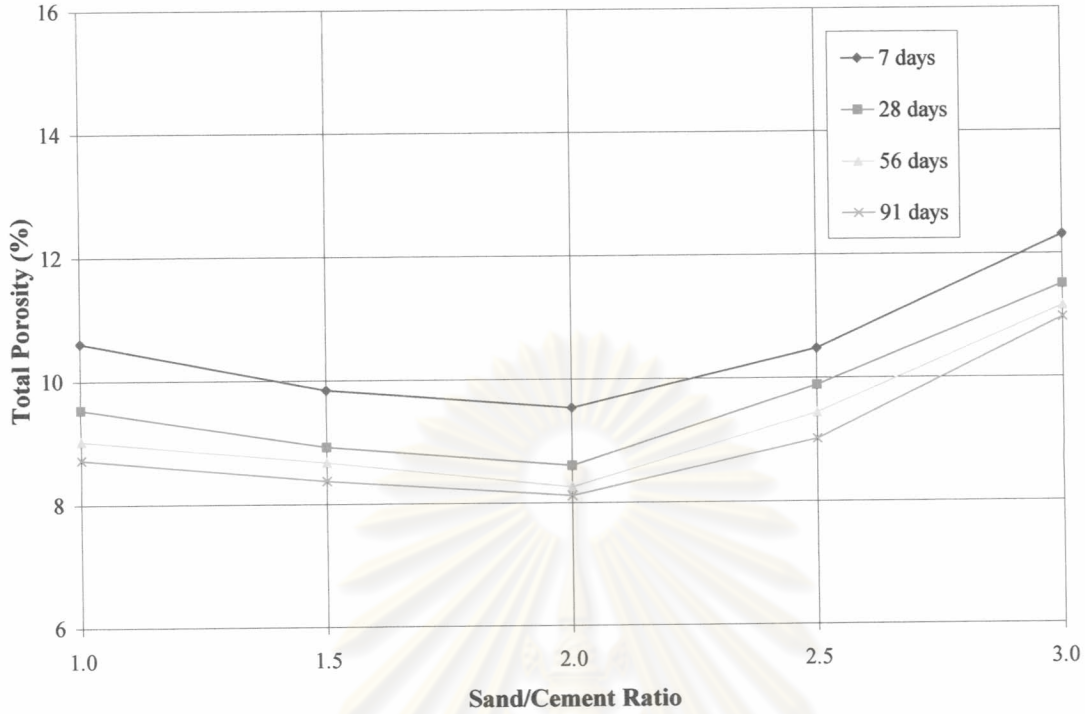

Fig. 4.7 Total porosity of mortar with various sand/cement ratio

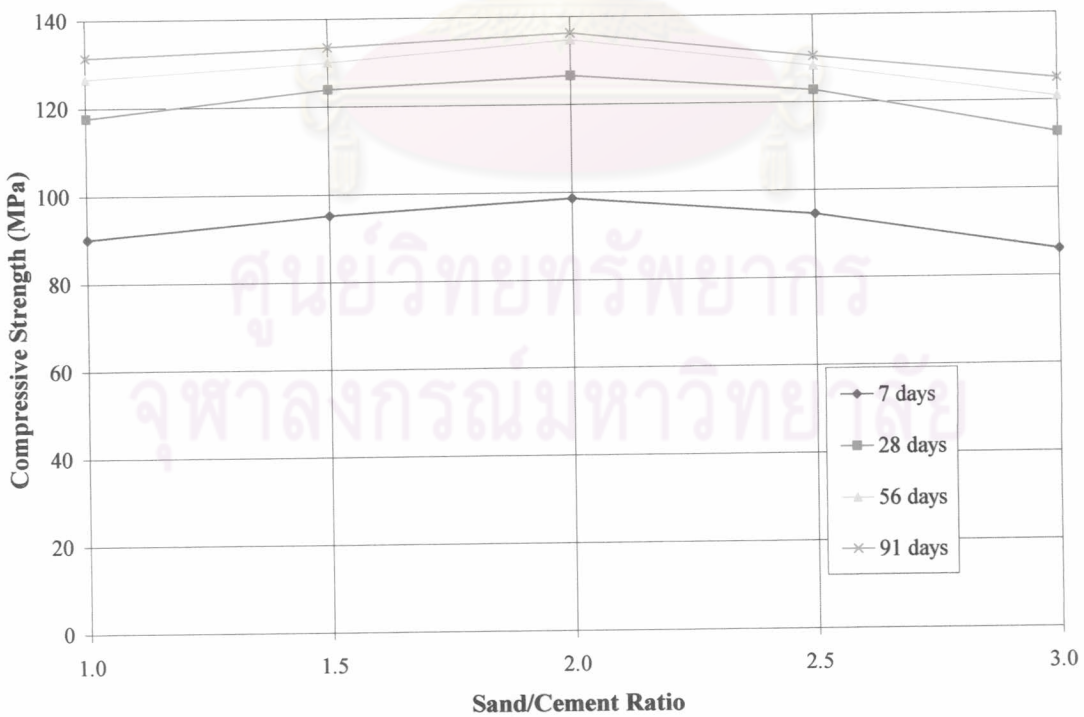

Fig. 4.8 Compressive strength of mortar with various sand/cement ratio

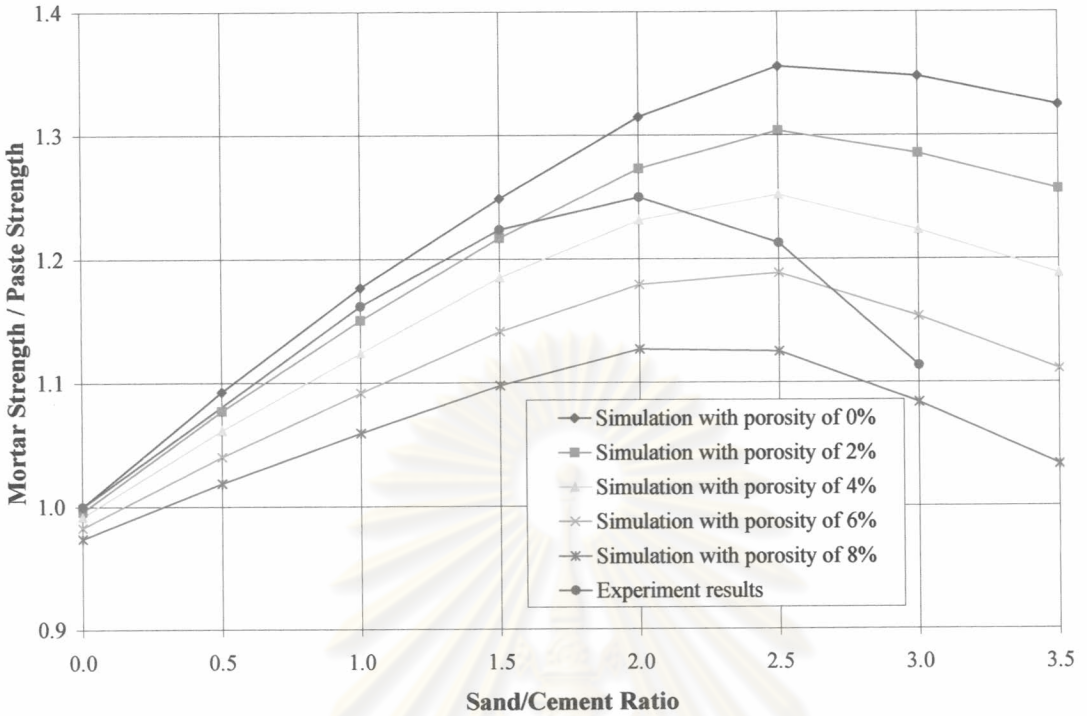

Fig. 4.9 *Comparison between ratio of mortar to paste strength from simulations and experiment*

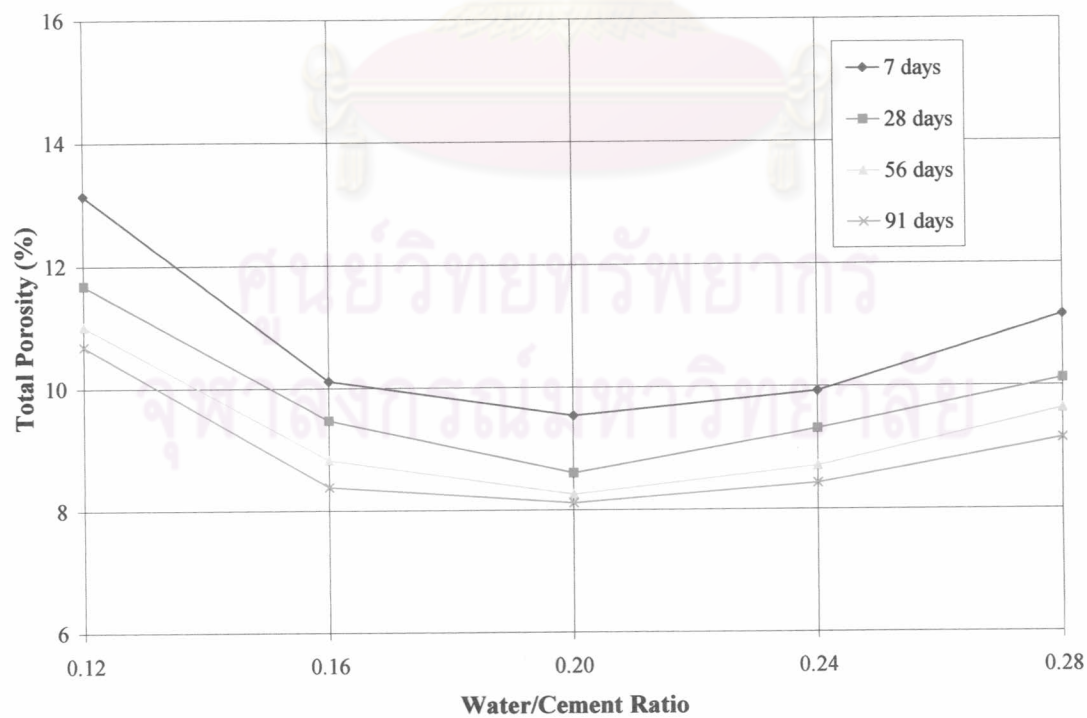

Fig. 4.10 *Total porosity of mortar with various water/cement ratio*

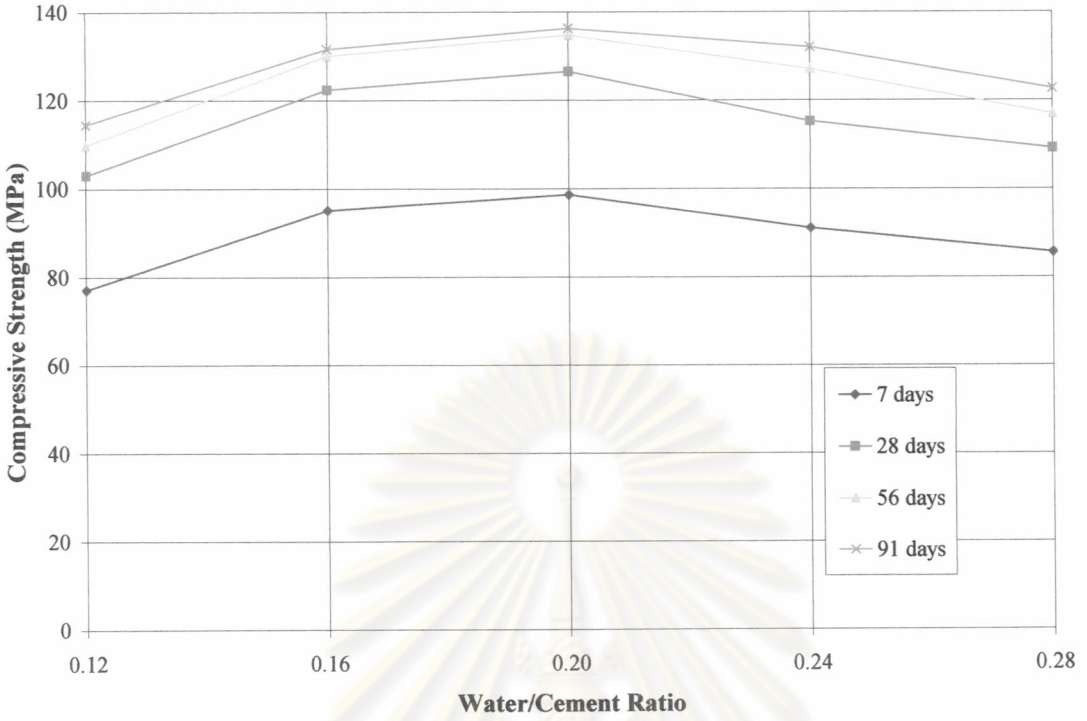

Fig. 4.11 *Compressive strength of mortar with various water/cement ratio*